Solving the Generalized Poisson Equation Using the Finite-Difference Method (FDM)

James R. Nagel, nageljr@ieee.org
Department of Electrical and Computer Engineering
University of Utah, Salt Lake City, Utah

February 15, 2012

1   Introduction

The Poisson equation is a very powerful tool for modeling the behavior of electrostatic systems, but unfortunately may only be solved analytically for very simplified models. Consequently, numerical simulation must be utilized in order to model the behavior of complex geometries with practical value. Although there are several competing algorithms for achieving this goal, one of the simplest and more straightforward of these is called the *finite-difference method* (FDM). At its core, FDM is nothing more than a direct conversion of the Poisson equation from continuous functions and operators into their discretely-sampled counterparts. This converts the entire problem into a system of linear equations that may be readily solved via matrix inversion. The accuracy of such a method is therefore directly tied to the ability of a finite grid to approximate a continuous system, and errors may be arbitrarily reduced by simply increasing the number of samples.

Despite the relative simplicity of FDM as a numerical tool, information on the subject is surprisingly scarce. This is especially true for the case of quasi-static systems experiencing current flow in conducting materials. Part of the reason for this likely has to do with the fact that FDM is, at its core, nothing more than a simplified form of the finite element method (FEM). The only difference is that FDM is solved through a fixed, rectangular geometry, while FEM utilizes a flexible, triangular mesh. Nevertheless, the uniform grids inherent to FDM make it very intuitive to learn and to program, especially for students unfamiliar with techniques in numerical methods. Consequently, the learning curve for FEM is far steeper than it is for FDM, and often requires a whole semester of study to fully understand. On the other hand, expertise with FDM may be readily achieved in only a few weeks, and even serves as an intuitive springboard from which to study the more complex nature of FEM.

The goal of this paper is to serve as a comprehensive introduction to the principles of FDM. Much of the basic information is readily found in standard textbooks [1, 2], though many of the practical details and advanced topics are difficult to find anywhere at all. This paper is therefore a compilation of knowledge based on my experience with FDM, as well as a primer on some of the more advanced topics that are almost nonexistent in the literature. The audience is specifically intended to include first-year students in computational electromagnetics, but more advanced professionals should still find useful reference material as well. The basic governing equations are derived directly from Maxwell's equations and FDM is first introduced in its most basic formulation. The algorithm is then extended from the classical Poisson equation to the generalized Poisson equation in order to include the effects of varying dielectrics within the domain. Finally, we conclude with an extension

of FDM to include quasi-static systems by showing how the exact same governing equation still applies for complex-valued phasors.

2   The Generalized Poisson Equation

Beginning with Maxwell's equations, the ultimate governing equation for any electrostatic system is Gauss's law. Expressed in point form, this may be written as

$$\nabla \cdot \mathbf{D}(\mathbf{r}) = \rho(\mathbf{r}) \ . \tag{1}$$

In this context, $\mathbf{r} = x\hat{\mathbf{x}} + y\hat{\mathbf{y}} + z\hat{\mathbf{z}}$ is a position vector in space, ρ is the charge density function, and $\mathbf{D}$ is the electric flux density. Using the constitutive relation $\mathbf{D}(\mathbf{r}) = \epsilon_0 \epsilon(\mathbf{r})\mathbf{E}(\mathbf{r})$, Gauss's law may be rewritten in terms of the electric field intensity $\mathbf{E}$ as

$$\nabla \cdot \Big[\epsilon(\mathbf{r}) \ \mathbf{E}(\mathbf{r})\Big] = \frac{\rho(\mathbf{r})}{\epsilon_0} \ , \tag{2}$$

where $\epsilon(\mathbf{r})$ is the dielectric constant as a function of position in space and $\epsilon_0 = 8.854 \times 10^{-12}$ F/m is the permittivity of free-space. Gauss's law may be further rewritten in terms of the *voltage potential function* $V(\mathbf{r})$ by making the substitution $\mathbf{E}(\mathbf{r}) = -\nabla V(\mathbf{r})$:

$$\nabla \cdot \Big[\epsilon(\mathbf{r}) \ \nabla V(\mathbf{r})\Big] = -\frac{\rho(\mathbf{r})}{\epsilon_0} \ . \tag{3}$$

Although it is not commonly discussed in the literature, this is really nothing more than a generalized form of the *Poisson equation*, and is the expression we shall be most interested in throughout this paper. A far more familiar expression occurs if we next assume a uniform dielectric function with the form $\epsilon(\mathbf{r}) = \epsilon_r$. This gives us

$$\nabla^2 V(\mathbf{r}) = -\frac{\rho(\mathbf{r})}{\epsilon_0 \epsilon_r} \ , \tag{4}$$

which is the classical form for the Poisson equation as given in most textbooks.

Although the classical Poisson equation is much simpler to numerically solve, it also tends to be very limited in its practical utility. Realistically, the generalized Poisson equation is the true equation we will eventually need to solve if we ever expect to properly model complex physical systems. We shall therefore begin by using the classical Poisson equation as a demonstration case for how FDM works before expanding our algorithm to the generalized form. For brevity and simplicity, this paper will be strictly limited to two-dimensional systems, though a full three-dimensional solution follows a nearly identical derivation.

3   The Five-Point Star

The first step in applying FDM is to define a *mesh*, which is simply a uniform grid of spatial points at which the voltage function will be sampled. Letting h be the distance between each sample, the points that lie on the mesh may be defined by

$$x_i = ih \ , \quad \text{and} \tag{5}$$

$$y_j = jh \ , \tag{6}$$
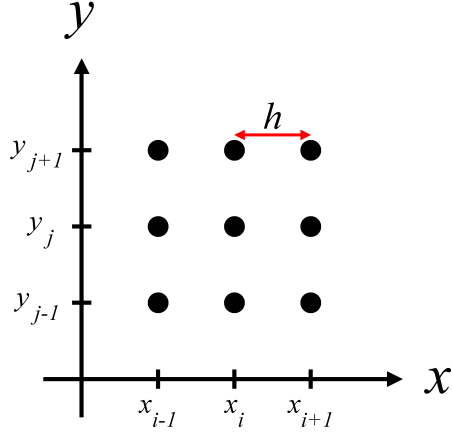
Figure 1: Mesh points for the FDM grid.

where i and j are integers. In practice, i and j will eventually be used as indices for a matrix of voltage samples, so it helps to use a short-hand notation that bears this in mind. We shall therefore replace the spatial coordinates with simple indices by assuming the following convention:

$$V(i,j) = V(x_i, y_j) . \tag{7}$$

In a similar fashion, we may also define the charge density samples along the same mesh by using the $\rho(i,j)$ notation.

The next step is to expand the Poisson equation by explicitly showing the partial derivatives in space:

$$\frac{\partial^2 V(i,j)}{\partial x^2} + \frac{\partial^2 V(i,j)}{\partial y^2} = -\frac{\rho(i,j)}{\epsilon_0} . \tag{8}$$

The reason for doing this is so that we may approximate the derivative operators through the use of finite-differences. The easiest way to do this is through the three-point approximation for the second-derivative, which is given as

$$\frac{\partial^2}{\partial x^2} V(i,j) \approx \frac{V(i-1,j) - 2V(i,j) + V(i+1,j)}{h^2} , \tag{9}$$

with a similar expression for the partial derivative with respect to y. Plugging back into Equation (8) then gives us

$$V(i-1,j) + V(i+1,j) + V(i,j-1) + V(i,j+1) - 4V(i,j) = -\frac{h^2}{\epsilon_0} \rho(i,j) . \tag{10}$$

Finally, we solve for $V(i,j)$ to find

$$V(i,j) = \frac{1}{4} \left[V(i-1,j) + V(i+1,j) + V(i,j-1) + V(i,j+1) + \frac{\rho(i,j)h^2}{\epsilon_0} \right] . \tag{11}$$

What this expression tells us is that every voltage sample $V(i,j)$ is dependent only on $\rho(i,j)$ and the voltage at the four nearest neighbors. A graphical depiction of this is called a *computational molecule*, and is shown in Figure 2. Because of its unique geometry, this five-point stencil is often referred to as the *five point star*.

3
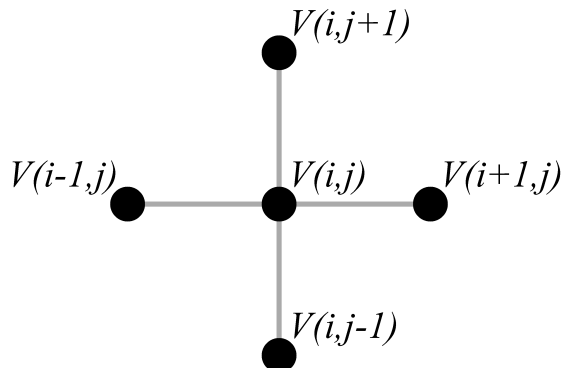
Figure 2: Computational molecule for the 5-point star.

Because each voltage sample $V(i,j)$ is linearly dependent on its four nearest neighbors, the solution over all (i,j) may be represented as a simple matrix-vector equation. This is readily achieved by defining the vector $\mathbf{x}$ to contain all of the voltage samples within the domain. For example, one simple method might scan row-wise along the voltage samples according to the convention:

$$\mathbf{x} = \begin{bmatrix} V(1,1) & V(1,2) & V(1,3) & \cdots & V(2,1) & V(2,2) & V(2,3) & \cdots \end{bmatrix}^T . \tag{12}$$

The next step is to express the linear relationship between voltage samples into a matrix $\mathbf{A}$. This effectively converts the entire problem into a matrix-vector equation with the form

$$\mathbf{A}\mathbf{x} = \mathbf{b} , \tag{13}$$

where $\mathbf{b}$ contains all the information about any charge densities and boundary conditions. The numerical solution to the system is finally found by simply inverting the matrix $\mathbf{A}$ to arrive at

$$\mathbf{x} = \mathbf{A}^{-1}\mathbf{b} . \tag{14}$$

4   Boundary Conditions

Because a computer can only store a finite number of grid points, it is always necessary to truncate a simulation domain along some fixed boundary. Since the five-point star is not applicable at the boundary samples, it is necessary to specify boundary conditions in order to arrive at a unique solution to the problem. The two most basic forms of boundary condition are called the *Dirichlet* boundary and the *Neumann boundary*. In practice, it is common for simulations to employ a mixture of these two conditions at the edges, so it is helpful to define Ω_D and Ω_N as the set of all points which satisfy the Dirichlet and Neumann conditions.

The simplest boundary condition is the Dirichlet boundary, which may be written as

$$V(\mathbf{r}) = f(\mathbf{r}) \qquad (\mathbf{r} \in \Omega_D) . \tag{15}$$

The function f is a known set of values that defines V along Ω_D. Thus, the Dirichlet boundary is nothing more than a forced solution to the potential function at specific points. A good example of such a condition occurs in the presence of charged metal plates. Because all points on a metal are
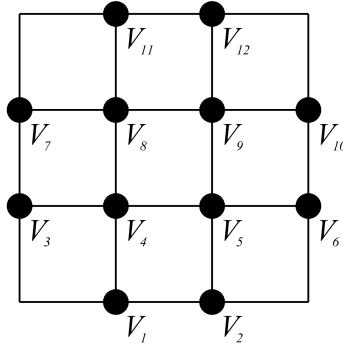
Figure 3: Sampled grid of voltages from Example 1.

at the same potential, a metal plate can readily be modeled by a region of points with some fixed voltage. In contrast, the Neumann boundary condition exists when the derivative of the potential function is known. Generally speaking, the derivative is defined with respect to the outward unit normal at the boundary, which is written as

$$\frac{\partial V(\mathbf{r})}{\partial \mathbf{n}} = f'(\mathbf{r}) \qquad (\mathbf{r} \in \Omega_N) \; , \tag{16}$$

where $\mathbf{n}$ is the outward-pointing unit normal vector, and f' the specifies the set of known derivatives. Unlike the Dirichlet condition, the Neumann does not offer a direct solution to the voltage potentials on a discrete, sampled grid. Rather, the boundary point must be expressed in terms of the surrounding points by applying a new stencil. The simplest method for expressing this is by imagining a central-difference approximation between the boundary sample V_b and the first inner sample V_i:

$$\frac{V_b - V_i}{h} = f' \; . \tag{17}$$

It is important to remember that the derivative function f' is defined with respect to the outward normal direction. This convention allows us to express Equation (17) the same way without any care for where exactly the boundary itself is located, be it top, bottom, left, or right of the simulation domain.

4.1 Example 1: A simple 4 × 4 grid

Consider the simple, 4 × 4 grid of voltage samples depicted in Figure 3. The top boundary is a Dirichlet boundary fixed at 1.0 V with bottom boundary grounded at 0.0 V. The left and right boundaries are Neumann boundaries fixed to a derivative of 0.0 V/m with respect to the outward normal. Using FDM, it is our job to solve for the voltage potentials at all of the indicated points.

The first step is to establish some sort of numbering convention so that the unknown vector $\mathbf{x}$ may be defined. One straightforward way to do this is by scanning across the rows, as indicated by the numbering in Figure 3. It is also worth emphasizing that the samples along the corners of the domain do not make any difference to the final solution of the problem with respect to the interior points. This is because neither the boundary conditions nor the five-point star will depend on what values are placed within the corners. We will therefore neglect these points entirely from the solution set, though in practice it can often be easier to just assign convenient values to them.[1] The

vector of unknowns will therefore be written as

$$\mathbf{x} = \begin{bmatrix} V_1 & V_2 & V_3 & \cdots & V_{12} \end{bmatrix}^T .$$

The next step is to fill the system matrix $\mathbf{A}$. We begin by noting that V_1 and V_2 are both Dirichlet boundaries fixed at 0.0 V. The first two rows in $\mathbf{A}$ are therefore nothing but zeros with a one placed at the diagonal element. The same is also true for V_{11} and V_{12} since these are likewise Dirichlet boundaries. The Neumann boundaries are filled in a similar manner, but with a -1 placed on the column corresponding to the interior point. For V_3 and V_7, this is the first element to the right of the diagonal. For V_6 and V_{10}, the -1 is placed at the first element to the left of the diagonal. For the remainder of the samples, the five-point star dictates a value of -4 to be placed at the diagonal, with four 1's placed at their corresponding columns that represent the neighboring points. This will include the two columns immediately adjacent to the diagonal, plus two other 1's placed at the appropriate locations.

The final step is to fill the forcing vector $\mathbf{b}$. Generally speaking, this will be a vector of all zeros except at the points where there is a nonzero boundary condition or a nonzero value for ρ. Thus, $\mathbf{b}$ has only two 1's placed in the last two rows, with zeros placed at all other elements. Writing out the full linear system $\mathbf{Ax} = \mathbf{b}$ therefore leads to

$$
\begin{bmatrix}
1 & 0 & 0 & 0 & 0 & 0 & 0 & 0 & 0 & 0 & 0 & 0 \\
0 & 1 & 0 & 0 & 0 & 0 & 0 & 0 & 0 & 0 & 0 & 0 \\
0 & 0 & 1 & -1 & 0 & 0 & 0 & 0 & 0 & 0 & 0 & 0 \\
1 & 0 & 1 & -4 & 1 & 0 & 0 & 1 & 0 & 0 & 0 & 0 \\
0 & 1 & 0 & 1 & -4 & 1 & 0 & 0 & 1 & 0 & 0 & 0 \\
0 & 0 & 0 & 0 & -1 & 1 & 0 & 0 & 0 & 0 & 0 & 0 \\
0 & 0 & 0 & 0 & 0 & 0 & 1 & -1 & 0 & 0 & 0 & 0 \\
0 & 0 & 0 & 1 & 0 & 0 & 1 & -4 & 1 & 0 & 1 & 0 \\
0 & 0 & 0 & 0 & 1 & 0 & 0 & 1 & -4 & 1 & 0 & 1 \\
0 & 0 & 0 & 0 & 0 & 0 & 0 & 0 & -1 & 1 & 0 & 0 \\
0 & 0 & 0 & 0 & 0 & 0 & 0 & 0 & 0 & 0 & 1 & 0 \\
0 & 0 & 0 & 0 & 0 & 0 & 0 & 0 & 0 & 0 & 0 & 1
\end{bmatrix}
\begin{bmatrix}
V_1 \\ V_2 \\ V_3 \\ V_4 \\ V_5 \\ V_6 \\ V_7 \\ V_8 \\ V_9 \\ V_{10} \\ V_{11} \\ V_{12}
\end{bmatrix}
=
\begin{bmatrix}
0 \\ 0 \\ 0 \\ 0 \\ 0 \\ 0 \\ 0 \\ 0 \\ 0 \\ 0 \\ 1 \\ 1
\end{bmatrix} .
$$

Finally, we solve for $\mathbf{x} = \mathbf{A}^{-1}\mathbf{b}$ to find

$$\mathbf{x} = \begin{bmatrix} 0 & 0 & \frac{1}{3} & \frac{1}{3} & \frac{1}{3} & \frac{1}{3} & \frac{2}{3} & \frac{2}{3} & \frac{2}{3} & \frac{2}{3} & 1 & 1 \end{bmatrix}^T \text{ Volts} .$$

5 Successive Over-Relaxation

For relatively small simulation domains, the direct matrix inversion demonstrated by the previous example works perfectly well for obtaining a solution. However, it is important to realize that the size of $\mathbf{A}$ grows directly with the *square* of the size of $\mathbf{x}$. For example, given a rectangular simulation domain of 100×100 voltage samples, the matrix $\mathbf{A}$ will need to be $10,000 \times 10,000$ elements. Because direct matrix inversion is such an intense operation, it is easy to see how even small simulations can quickly require excessive computational resources.

To reduce the computational cost required by direct matrix inversion, it helps to realize that $\mathbf{A}$ is a *sparse* matrix, meaning the vast majority of elements in $\mathbf{A}$ are all zeros. This is a direct

---

[1]Imagine a square simulation grid of 200×200 voltage samples. Is it really worth the effort to write a specialized algorithm just to save memory on four measly samples?

consequence of Equation (11), which shows that each voltage element is only dependent on four other samples. As a result, each row in $\mathbf{A}$ has, at most, only five nonzero entries (or even one nonzero entry if the voltage sample is a fixed Dirichlet boundary). This allows us arrive at a solution through the use of sparse matrix solvers that take take advantage of this property. Although there are many available methods to chose from [3], we will focus on a very simple algorithm called *successive over-relaxation* (SOR).

The first step when utilizing SOR is to define the *residual* $R(i, j)$ as the degree to which each voltage sample $V(i, j)$ does not satisfy Equation (11):

$$R(i,j) = \frac{1}{4}\left[V(i-1,j) + V(i+1,j) + V(i,j-1) + V(i,j+1) + \frac{\rho(i,j)h^2}{\epsilon_0}\right] - V(i,j) \qquad (18)$$

The next step is to loop over every sample in $V(i, j)$ and add a correction factor defined by $R(i, j)$. This process is then repeated over many iterations until the residual falls below some acceptable error value. For the kth iteration in the loop, we therefore have

$$V^{k+1}(i,j) = V^k(i,j) + R^k(i,j) \ . \qquad (19)$$

This method is referred to as *successive relaxation*, and is guaranteed to eventually converge on the correct solution.

Although convergence is a desirable property of successive relaxation, a far more practical property is *rapid* convergence. This may be achieved if we first multiply R with a *relaxation factor* ω, such that

$$V^{k+1}(i,j) = V^k(i,j) + \omega R^k(i,j) \ . \qquad (20)$$

This is called the method of successive *over*-relaxation, and will also converge as long as we enforce the condition that $0 < \omega < 2$. The only tricky part is choosing an ideal value for ω that minimizes the time to convergence. Generally speaking, this can only be found through empirical trial-and-error, but a special case arises for rectangular grids. The proof of this is rather involved, so we shall simply state the end result from [1] as

$$\omega = \frac{8 - \sqrt{64 - 16t^2}}{t^2} \ , \qquad (21)$$

where N_x and N_y are the number of grid samples in the x- and y-directions, and

$$t = \cos(\pi/N_x) + \cos(\pi/N_y) \ . \qquad (22)$$

6   Electric Fields

From the basic definition $\mathbf{E} = -\nabla V$, it is a straightforward process to extract electric fields from a complex simulation of voltage potentials. We therefore begin by expanding the definition of the gradient into its constituent x and y components:

$$\mathbf{E}(\mathbf{r}) = -\hat{\mathbf{x}}\frac{\partial V(\mathbf{r})}{\partial x} - \hat{\mathbf{y}}\frac{\partial V(\mathbf{r})}{\partial y} \ . \qquad (23)$$

The next step is to apply the central difference approximation to the individual field components. The resulting grid of electric field samples is therefore slightly staggered from the voltage potentials
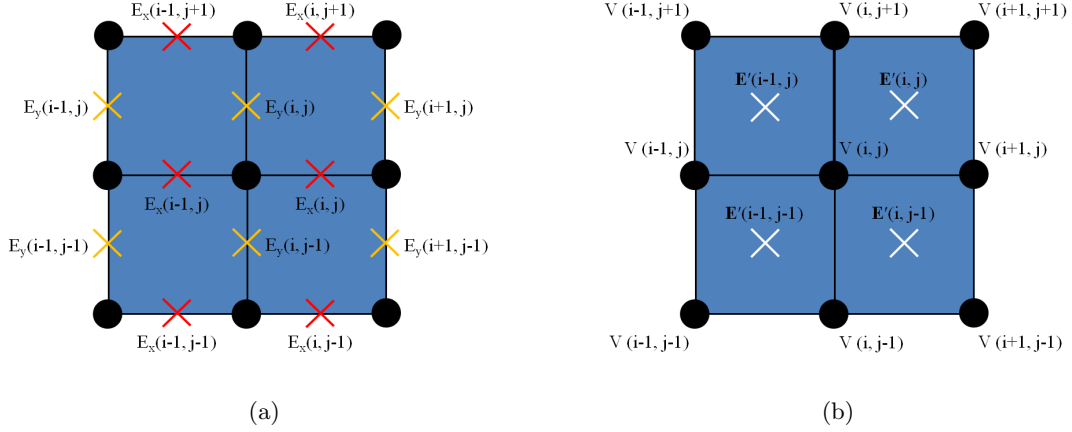
Figure 4: Grid stencil for obtaining the electric field samples. Circles represent voltage samples while ×'s represent the electric field samples. (a) Central differences are first calculated individually along the x and y directions, (b) then averaged together to produce a field sample that is staggered from the voltage grid.

according to the convention shown in Figure 4(a). These components are thus given as

$$E_x(i, j) = -\frac{V(i+1, j) - V(i, j)}{h} \ , \tag{24}$$

$$E_y(i, j) = -\frac{V(i, j+1) - V(i, j)}{h} \ . \tag{25}$$

At this point, two points of information are worth noting. The first is that the E_x grid contains one fewer sample along the x-direction than does the V grid. Similarly, the E_y grid is comprised of one fewer sample along the y-direction. This is simply a natural result of applying the central-difference method to compute a numerical derivative. The second point is that the x- and y-components of the electric field are staggered from each other in space. In order to fix this, we must apply a second approximation by averaging the field components together according to the geometry in Figure 4(b). Letting E_x' and E_y' represent the new set of grid samples, this is written as

$$E_x'(i, j) = \frac{1}{2} \Big[E_x(i, j+1) + E_x(i, j) \Big] \ , \tag{26}$$

$$E_y'(i, j) = \frac{1}{2} \Big[E_y(i+1, j) + E_y(i, j) \Big] \ . \tag{27}$$

Thus, the electric field components are now placed at the same grid locations by defining them along a staggered grid from the voltage potentials. As we shall see in Section 7, such an arrangement also avoids any of the confusion that occurs at the boundaries between dielectric surfaces, since normal field components may be discontinuous here. Finally, the number of rows and columns in the E-field grid are both one less than those of the voltage grid.

6.1 Example 2: The Parallel Plate Capacitor

One of the more interesting simulations readily employed by FDM is the parallel plate capacitor. A demonstration of this scenario is depicted in Figure 5. The simulation domain size was set to 230×135 grid samples, thus giving an over-relaxation constant of $\omega \approx 1.96$. The error bound was

<div align="center">(a)   (b)</div>
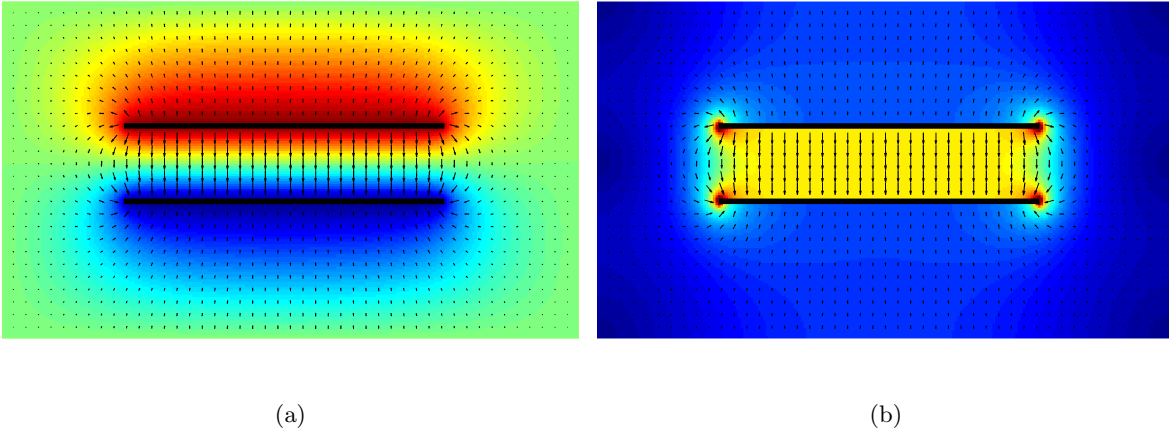
Figure 5: A 2D parallel-plate capacitor. The top plate is at a potential of $+1.0$ V while the bottom plate is at -1.0 V. The color mapping represents (a) the voltage potential and (b) the electric field intensity. Quiver plots represent electric field vectors.

set to a value of 10^{-6} and required 427 iterations to converge. The capacitor plates were defined as a set of Dirichlet boundaries fixed at a potential of $+1.0$ V for the top plate and -1.0 V for the bottom plate,[2] with 0.0 V for the simulation boundaries. The color map in Figure 5(a) represents the voltage potential, with a quiver plot superimposed to represent the electric field vectors. The color map in Figure 5(b) represents the magnitude of the electric field itself. To reduce the effects of the simulation boundaries on the fields near the capacitor, the simulation boundaries were placed many grid points away from the plates as an approximation to a free-space environment.

7 Varying Dielectrics

Let us now return to the generalized Poisson equation:

$$\nabla \cdot \left[\epsilon(\mathbf{r}) \, \nabla V(\mathbf{r}) \right] = -\frac{\rho(\mathbf{r})}{\epsilon_0} \; . \tag{28}$$

Although it is tempting to begin by directly applying numerical derivatives to this expression, a far more accurate method may be derived if we first realize that $\epsilon(\mathbf{r})$ does not necessarily need to be sampled at identical grid points as $V(\mathbf{r})$. We shall therefore begin by defining the permittivities as sectionally constant regions along the *staggered* grid shown in Figure 6. Mathematically, this may be written as

$$\epsilon(i,j) = \epsilon(x_i + h/2, y_j + h/2) \; , \tag{29}$$

with $V(i,j)$ and $\rho(i,j)$ defined along the original grid points as before. Defining the permittivities in this way has two important advantages. First, it allows us to define the voltage samples along the boundaries of the dielectric permittivities. This is important when we compute the electric fields from the voltage samples, since electric fields are discontinuous at planar boundaries. The second, and more important reason, is that it allows us to exploit the properties of variational calculus by expressing Equation (28) in its *weak*, or *variational*, form. In so doing, the second-order derivatives vanish and leave only first-order derivatives for us to numerically approximate.

---

[2]Notice how Dirichlet conditions can also be defined at interior points within the simulation domain and are not limited just to the external boundaries.
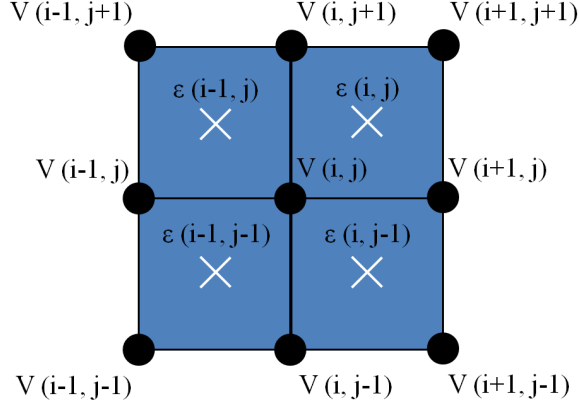
Figure 6: Finite-difference mesh for the generalized Poisson equation. Each blue square represents a region of constant dielectric permittivity.

We begin by defining Ω_{ij} as the square region around a single voltage sample $V(i,j)$, as depicted in Figure 7(a). We then take the surface integral around Ω_{ij} to find

$$\iint\limits_{\Omega_{ij}} \nabla \cdot \left[\epsilon(\mathbf{r}) \, \nabla V(\mathbf{r})\right] d\Omega = -\frac{1}{\epsilon_0} \iint\limits_{\Omega_{ij}} \rho(\mathbf{r}) \, d\Omega \, , \tag{30}$$

where $d\Omega = dxdy$ is the differential surface area. Looking first at the right-hand side of Equation (30), we note that the integral over the charge density is simply the total charge enclosed by Ω_{ij}. We may therefore make the replacement

$$-\iint\limits_{\Omega_{ij}} \rho(\mathbf{r}) \, d\Omega = -Q(i,j) \, . \tag{31}$$

The left-hand side of Equation (30) may also be simplified by applying the divergence theorem. This converts the surface integral over Ω_{ij} into a contour integral around its outer border, thus giving

$$\iint\limits_{\Omega_{ij}} \nabla \cdot \left[\epsilon(\mathbf{r}) \, \nabla V(\mathbf{r})\right] d\Omega = \oint\limits_{C_{ij}} \left[\epsilon(\mathbf{r}) \, \nabla V(\mathbf{r})\right] \cdot d\mathbf{n} \, . \tag{32}$$
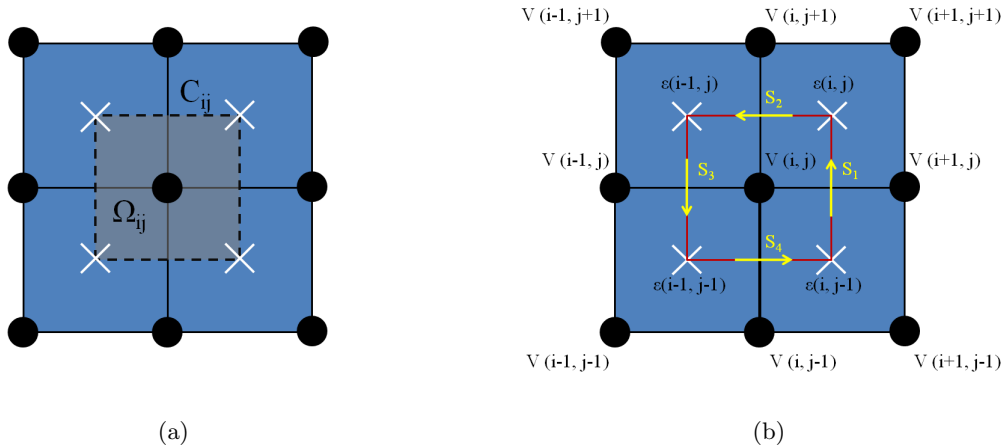
where C_{ij} is the enclosing contour and $d\mathbf{n}$ is the differential unit normal vector. The end result is therefore

$$\oint\limits_{C_{ij}} \left[\epsilon(\mathbf{r}) \, \nabla V(\mathbf{r})\right] \cdot d\mathbf{n} = -\frac{Q(i,j)}{\epsilon_0} \, . \tag{33}$$

This expression is referred to as the *weak form* of Poisson's equation, while Equation (28) is called the *strong form.*

With the desired expression in hand, the next step is to expand out the gradient operator to find

$$\oint\limits_{C_{ij}} \left[\epsilon(\mathbf{r}) \, \nabla V(\mathbf{r})\right] \cdot d\mathbf{n} = \oint\limits_{C_{ij}} \left[\epsilon(\mathbf{r}) \left(\frac{\partial}{\partial x}V(\mathbf{r})\hat{\mathbf{x}} + \frac{\partial}{\partial y}V(\mathbf{r})\hat{\mathbf{y}}\right)\right] \cdot d\mathbf{n} \tag{34}$$

Figure 7: The volume element Ω_{ij} surrounds the voltage sample $V(i,j)$. The outer contour C_{ij} encloses Ω_{ij} and defines the contour integral of Equation (32) in the counter-clockwise direction.

Note that in three dimensions, the surface C_{ij} would normally be a cube, but in our two-dimensional example is simply a square contour. The total contour integral my therefore be broken down by treating it as a series of sub-integrals around each side of the square. For brevity, we shall simply write these integrals as $S_1 \cdots S_4$:

$$\oint_{C_{ij}} \left[\epsilon(\mathbf{r}) \left(\frac{\partial}{\partial x} V(\mathbf{r})\hat{\mathbf{x}} + \frac{\partial}{\partial y} V(\mathbf{r})\hat{\mathbf{y}} \right) \right] \cdot d\mathbf{n} = \int_{S_1} + \int_{S_2} + \int_{S_3} + \int_{S_4} . \tag{35}$$

This geometry is depicted in Figure 7(b), which highlights the contour of integration over all four sides, taken in the counter-clockwise direction.

To begin, let us define S_1 as the right edge of the square where $d\mathbf{n} = \hat{\mathbf{x}}\, dy$. For convenience, it also helps to assume that $V(i,j)$ lies at the origin, though the end result will be equivalent no matter what location we choose. We may therefore express the integral over S_1 as

$$\int_{S_1} = \int_{-h/2}^{h/2} \epsilon(x,y) \left(\frac{\partial}{\partial x} V(x,y)\,\hat{\mathbf{x}} + \frac{\partial}{\partial y} V(x,y)\,\hat{\mathbf{y}} \right) \cdot \hat{\mathbf{x}}\, dy = \int_{-h/2}^{h/2} \epsilon(x,y) \frac{\partial}{\partial x} V(x,y)\, dy . \tag{36}$$

Next, we note that the contour integral is taken entirely along the border between the regions defined by $V(i,j)$ and $V(i+1,j)$. We may therefore approximate the partial derivative by using a central difference between the two samples and then assume it remains constant across the entire border. Calculating the integral across the two dielectric regions therefore gives

$$\int_{S_1} \approx h \left[\frac{\epsilon(i,j) + \epsilon(i,j-1)}{2} \right] \left[\frac{V(i+1,j) - V(i,j)}{h} \right]$$

$$= (1/2) \left[\epsilon(i,j) + \epsilon(i,j-1) \right] \left[V(i+1,j) - V(i,j) \right] . \tag{37}$$

11

Carrying out this same operation over the other three sides thus gives

$$\int_{S_2} \approx (1/2) \left[\epsilon(i-1,j) + \epsilon(i,j) \right] \left[V(i,j+1) - V(i,j) \right] \tag{38}$$

$$\int_{S_3} \approx (1/2) \left[\epsilon(i-1,j-1) + \epsilon(i-1,j) \right] \left[V(i-1,j) - V(i,j) \right] \tag{39}$$

$$\int_{S_4} \approx (1/2) \left[\epsilon(i,j-1) + \epsilon(i-1,j-1) \right] \left[V(i,j-1) - V(i,j) \right] . \tag{40}$$

For notational compactness, we now define the following constants:

$$a_0 = \epsilon(i,j) + \epsilon(i-1,j) + \epsilon(i,j-1) + \epsilon(i-1,j-1)$$
$$a_1 = (1/2) \left[\epsilon(i,j) + \epsilon(i,j-1) \right]$$
$$a_2 = (1/2) \left[\epsilon(i-1,j) + \epsilon(i,j) \right]$$
$$a_3 = (1/2) \left[\epsilon(i-1,j-1) + \epsilon(i-1,j) \right]$$
$$a_4 = (1/2) \left[\epsilon(i,j-1) + \epsilon(i-1,j-1) \right] .$$

Finally, we put it all together to find

$$\oint_{C_{ij}} \approx -a_0 V(i,j) + a_1 V(i+1,j) + a_2 V(i,j+1) + a_3 V(i-1,j) + a_4 V(i,j-1) . \tag{41}$$

Including the charge term from Equation (33), we finally arrive at

$$\boxed{-a_0 V(i,j) + a_1 V(i+1,j) + a_2 V(i,j+1) + a_3 V(i-1,j) + a_4 V(i,j-1) = -\frac{Q(i,j)}{\epsilon_0}} . \tag{42}$$

Just like Equation (11), this expression represents a numerical stencil for the generalized Poisson equation. It is therefore a straightforward matter to generate a system of linear equations of the form $\mathbf{Ax} = \mathbf{b}$. However, just like before, $\mathbf{A}$ is a very large and sparse matrix, thereby making direct inversion a difficult option. Fortunately, the same procedure of successive over-relaxation can be applied to iteratively find a solution. Like before, we begin by solving for $V(i,j)$:

$$V(i,j) = \frac{1}{a_0} \left[a_1 V(i+1,j) + a_2 V(i,j+1) + a_3 V(i-1,j) + a_4 V(i,j-1) + \frac{Q(i,j)}{\epsilon_0} \right] . \tag{43}$$

We next define the residual as

$$R(i,j) = \frac{1}{a_0} \left[a_1 V(i+1,j) + a_2 V(i,j+1) + a_3 V(i-1,j) + a_4 V(i,j-1) + \frac{Q(i,j)}{\epsilon_0} \right] - V(i,j) . \tag{44}$$

And once again, the iteration formula is exactly as we found before:

$$V^{k+1}(i,j) = V^k(i,j) + \omega R^k(i,j) . \tag{45}$$

At this point, a word of warning should be emphasized about the use of SOR in regions with multiple dielectrics. Because of the scaling effects of the dielectric constants, SOR tends to converge more slowly as the dielectric constant is increased over some region. As a general rule, the
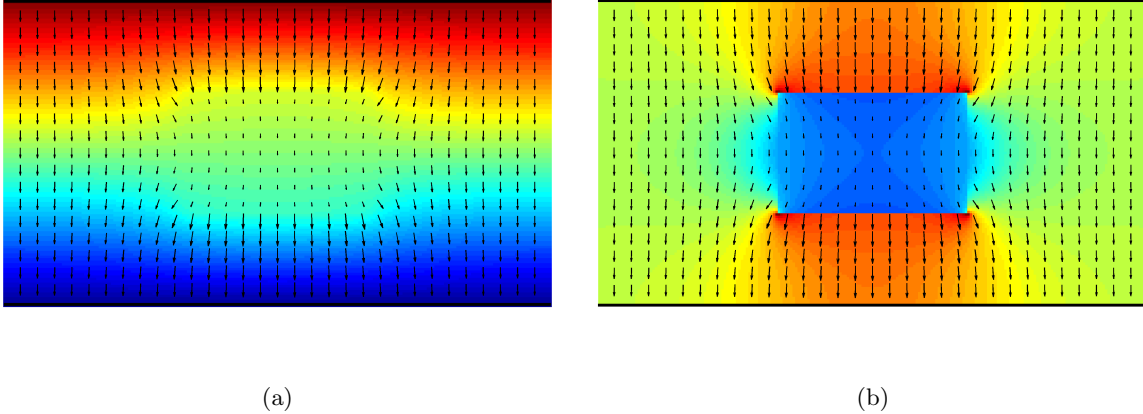
Figure 8: A 2D parallel-plate capacitor with a dielectric block ($\epsilon_r = 4$) placed inside. The color maps represent (a) voltage potential and (b) electric field intensity.

convergence rate of SOR will tend to be inversely linear with the maximum dielectric constant in the simulation domain. Thus, for regions with very high dielectrics, the SOR algorithm may even prematurely terminate before converging onto an accurate solution. In these situations, more advanced matrix solvers should be preferred over SOR for both speed and accuracy. However, such topics are beyond the scope of this paper and best left to a more advanced study of inversion theory and numerical methods [3].

7.1 Example 3: Dielectric Block in a Capacitor

Using FDM, simulate a parallel-plate capacitor with a dielectric block placed in between the plates. Use Dirichlet boundaries at the top and bottom with potentials of ± 1.0 V. Use Neumann boundaries at the left and right by setting the normal derivative to zero. Use a dielectric constant of $\epsilon_r = 4$ for the block.

Figure 8 shows an example simulation with the stated parameters. The block is centered between the plates with an aspect ratio of roughly 1.57. The color mapping in Figure 8(a) depicts the voltage potentials while Figure 8(b) depicts the electric field intensity. It is interesting to see how the voltage potential is relatively unperturbed by the presence of the block, while the electric field intensity is dramatically reduced inside the dielectric. The system matrix was inverted by using Matlab's matrix division operator ("\"), which computes quick and accurate inversion of sparse matrices.

8 Quasi-Static Systems

Another useful application for FDM is the ability to solve for quasi-static current density in conductive materials. We begin with Ampere's law in the frequency domain, which is written as

$$\nabla \times \mathbf{H}(\mathbf{r}) = j\omega\epsilon_0\epsilon(\mathbf{r})\,\mathbf{E}(\mathbf{r}) + \mathbf{J}_c(\mathbf{r}) + \mathbf{J}_i(\mathbf{r}) \ , \tag{46}$$

where $\mathbf{H}$ is the magnetic field intensity, $\mathbf{J}_c$ is the induced conduction current, and $\mathbf{J}_i$ is an impressed current source. At this point, the reader should bear in mind that all functions are complex-valued phasors. We also use $j = \sqrt{-1}$ to denote the imaginary unit, and should not to be confused with

13

an integer index. The conduction current $\mathbf{J}_c$ represents any motion of charges that are due to the flow of electrons on a conductive material in the presence of an external electric field. These are computed from the point form of Ohm's law, which is given as

$$\mathbf{J}_c(\mathbf{r}) = \sigma(\mathbf{r})\,\mathbf{E}(\mathbf{r}) \; , \tag{47}$$

where σ is the material conductivity. The $\mathbf{J}_i$ term is an arbitrary mathematical forcing function that represents the flow of electrical currents impressed into the system by external agents. As we shall see shortly, $\mathbf{J}_i$ plays the role of the "source" term that ρ played in the static case.

A common trick in electromagnetics is to merge the displacement current and conduction current of Ampere's law into a single, complex quantity. This is accomplished by defining the *complex permittivity* ϵ_c through the relation

$$\epsilon_c(\mathbf{r}) = \epsilon(\mathbf{r}) + \frac{\sigma(\mathbf{r})}{j\omega\epsilon_0} \; . \tag{48}$$

From here, Ampere's law may now be expressed as

$$\nabla \times \mathbf{H}(\mathbf{r}) = j\omega\epsilon_0\epsilon_c(\mathbf{r})\,\mathbf{E}(\mathbf{r}) + \mathbf{J}_i(\mathbf{r}) \; . \tag{49}$$

If we now take the divergence of Ampere's law, the curl term on the left vanishes, leaving

$$\nabla \cdot \Big[\epsilon_c(\mathbf{r})\,\mathbf{E}(\mathbf{r})\Big] = -\frac{1}{j\omega\epsilon_0}\nabla \cdot \mathbf{J}_i(\mathbf{r}) \; . \tag{50}$$

Finally, we apply the *charge continuity equation* by replacing $j\omega\tilde{\rho} = -\nabla \cdot \mathbf{J}_i$ to arrive at

$$\nabla \cdot \Big[\epsilon_c(\mathbf{r})\,\mathbf{E}(\mathbf{r})\Big] = \frac{\tilde{\rho}(\mathbf{r})}{\epsilon_0} \; . \tag{51}$$

Note how this is identical to the form of Equation (2), but with a complex permittivity instead of real-valued. The tilde (˜) over the charge-density term is simply a reminder that ρ is now a complex phasor quantity rather than a real, static value.

Because we are now working with a time-varying system, it is important to realize that the electric field no longer satisfies the simple definition $\mathbf{E} = -\nabla V$. To see why, we must examine Faraday's law, which states

$$\nabla \times \mathbf{E}(\mathbf{r}) = -j\omega\mathbf{B}(\mathbf{r}) \; , \tag{52}$$

where $\mathbf{B} = \mu\mathbf{H}$ is the magnetic flux density. We now define a vector field $\mathbf{A}$ called the *magnetic vector potential* that satisfies

$$\mathbf{B}(\mathbf{r}) = \nabla \times \mathbf{A}(\mathbf{r}) \; . \tag{53}$$

Plugging back into Faraday's law therefore gives

$$\nabla \times \Big[\mathbf{E}(\mathbf{r}) + j\omega\mathbf{A}(\mathbf{r})\Big] = 0 \; . \tag{54}$$

The significance of this expression comes from an identity in vector calculus, which states that if the curl of some vector field is zero, then that field may be defined as the gradient of some undetermined scalar field V. In other words, V satisfies

$$\mathbf{E}(\mathbf{r}) + j\omega\mathbf{A}(\mathbf{r}) = -\nabla V(\mathbf{r}) \; . \tag{55}$$

14

This is the complete definition for voltage potential, and includes both the effects of an external electric field as well as a time-varying magnetic field. It also means that $\mathbf{E}$ must satisfy

$$\mathbf{E}(\mathbf{r}) = -\nabla V(\mathbf{r}) - j\omega\mathbf{A}(\mathbf{r}) \ . \tag{56}$$

Although it is possible to independently solve for both $\mathbf{A}$ and V to find $\mathbf{E}$, the process is extremely difficult and requires a very complex linear system to couple the two quantities together [4]. To avoid this complication, a far more simplified system may be reached if we impose the *quasi-static* approximation:

$$j\omega\mathbf{A}(\mathbf{r}) \approx 0 \ . \tag{57}$$

In other words, the contribution of $\mathbf{A}$ to the total electric field is negligible at low frequencies, and $\mathbf{E} \approx -\nabla V$. This allows us to rewrite Equation (51) as

$$\boxed{\nabla \cdot \left[\epsilon_c(\mathbf{r}) \ \nabla V(\mathbf{r}) \right] = -\frac{\tilde{\rho}(\mathbf{r})}{\epsilon_0}} \ . \tag{58}$$

Notice how Equation (58) is simply the generalized Poisson equation again, but with complex numbers now instead of purely real. The same FDM algorithm we have just learned may therefore be used to find low-frequency potentials in a time-varying system. The complex values representing V therefore capture the effects of phase shifts due to material conductivity or any arbitrary offsets impressed within $\tilde{\rho}$. Just like before, large values in the dielectric function do not converge well when using SOR, and so more advanced methods are recommended for inverting the resultant linear system $\mathbf{Ax} = \mathbf{b}$. The only restriction is that the frequency must be low enough such that the magnetic vector potential does not contribute any significant values to the electric field.

## 8.1   Example 4: Finite Conductors Excited by Constant Voltage

Using the complex-valued FDM, simulate a parallel-plate capacitor with two wires feeding the plates. Excite the plates with a single point of voltage at the tip of each wire. Use a conductivity of $\sigma = 10$ S/m for the metal and a frequency of $f = 1.0$ MHz. Assume the grid spacing is $h = 1.0$ mm. Plot the electric field intensity $\mathbf{E}$ and the conduction current density $\mathbf{J}_c$ of the simulation domain.

The results of this simulation are shown in Figure 9. The excitation voltage of the plates was set by defining a single grid point at the tip of each wire as a Dirichlet boundary. The top plate is excited by a $+1.0$ V point and the bottom plate is excited by a -1.0 V point. Because the output voltage is now a time-varying quantity, it is necessary to choose a point in time (say, $t = 0$) before converting the phasors into an instantaneous, time-domain value. The image in Figure 9(a) clearly shows the typical capacitor plate behavior, with virtually zero electric fields inside the actual metal of the plates. The excitation voltage is therefore nearly constant across both capacitor plates, as we should expect them to behave. The image in Figure 9(b) shows the current density of the same system as calculated from Equation (47). In this case, the single point of voltage excitation becomes apparent, as all the current either enters or exits from these two Dirichlet voltage samples. We can also readily see the behavior of the electrical currents as they flow along the inside of the plates.

9   Static Magnetic Fields

Let us now turn our attention to the problem of static magnetic field intensity. Recall from the previous section that we indirectly defined the magnetic vector potential using

$$\mathbf{B}(\mathbf{r}) = \nabla \times \mathbf{A}(\mathbf{r}) \ , \tag{59}$$

(a)   (b)
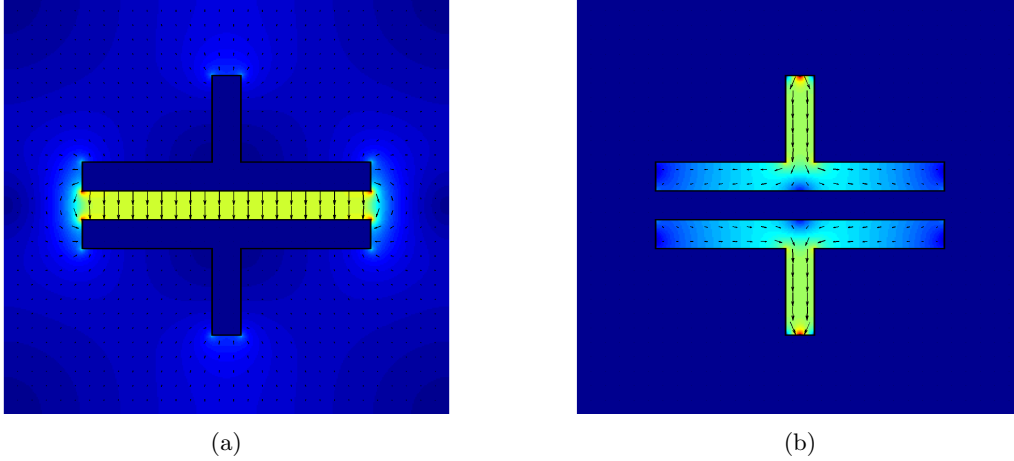
Figure 9: A 2D parallel-plate capacitor with feed-lines. Excitation of the feed-lines was achieved by a single Dirichlet boundary point ($V = \pm 1.0$ V) at the center of each tip. The complex dielectric constant of the metal plates was set to $\epsilon_c = 1 - j1.8 \times 10^5$.

where $\mathbf{B} = \mu \mathbf{H}$. For this problem, we shall even allow for the presence of magnetic materials by defining permeability function as

$$\mu(\mathbf{r}) = \mu_0 \mu_r(\mathbf{r}) \ , \tag{60}$$

where μ_0 is the permeability of free space and μ_r is relative permeability function. Taking the curl of Equation (59) and applying Ampere's law then leads us to the expression

$$\nabla \times \nabla \times \mathbf{A}(\mathbf{r}) = j\omega \mu_0 \epsilon_0 \mu_r(\mathbf{r})\epsilon_c(\mathbf{r})\, \mathbf{E}(\mathbf{r}) + \mu_0 \mu_r(\mathbf{r})\mathbf{J}_i(\mathbf{r}) \ . \tag{61}$$

For the case of static electric currents, the frequency of excitation is given by $\omega = 0$. We may therefore simplify this expression to read

$$\nabla \times \nabla \times \mathbf{A}(\mathbf{r}) = \mu_0 \mu_r(\mathbf{r})\mathbf{J}_i(\mathbf{r}) \ . \tag{62}$$

Although the double curl operation may look complex, it is possible to simplify matters by remembering the vector identity

$$\nabla \times \nabla \times \mathbf{A}(\mathbf{r}) = \nabla(\nabla \cdot \mathbf{A}(\mathbf{r})) - \nabla^2 \mathbf{A}(\mathbf{r}) \ . \tag{63}$$

It is also important to remember that we have not yet uniquely defined an exact value for $\mathbf{A}$. Instead, all we have done is indirectly define the magnetic vector potential as some unknown vector function such that taking the curl of $\mathbf{A}$ produces $\mathbf{B}$. This does not actually define $\mathbf{A}$ uniquely unless we first provide a *gauge*, or a value set by the divergence $\nabla \cdot \mathbf{A}$. Since we are still technically free to define $\mathbf{A}$ in any way we choose, it helps to choose a gauge that is convenient for a specific problem at hand. In this specific case, the most convenient value is called the *Coulomb gauge*, given by

$$\nabla \cdot \mathbf{A}(\mathbf{r}) = 0 \ . \tag{64}$$

Plugging this back into Equation (62) then produces

$$\boxed{\nabla^2 \mathbf{A}(\mathbf{r}) = -\mu_0 \mu_r(\mathbf{r})\mathbf{J}_i(\mathbf{r})} \ , \tag{65}$$

16
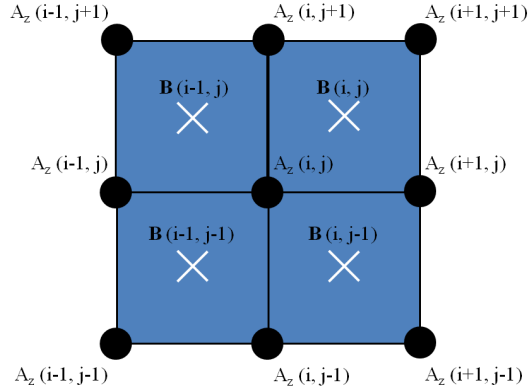
Figure 10: Grid stencil for obtaining the magnetic field samples .

which is nothing more than a vector form of the Poisson equation again. Breaking this up into vector components therefore reveals a set of three independent Poisson equations along each coordinate axis:

$$\nabla^2 A_x(\mathbf{r}) = -\mu_0 \mu_r(\mathbf{r}) J_x(\mathbf{r}) \tag{66}$$

$$\nabla^2 A_y(\mathbf{r}) = -\mu_0 \mu_r(\mathbf{r}) J_y(\mathbf{r}) \tag{67}$$

$$\nabla^2 A_z(\mathbf{r}) = -\mu_0 \mu_r(\mathbf{r}) J_z(\mathbf{r}) \ . \tag{68}$$

The full solution for $\mathbf{A}$ in three dimensions can therefore be found by independently solving each expression along its respective coordinate axis.

For the special case of two-dimensional systems, we may assume that $A_x = A_y = 0$ and limit ourselves strictly to the special case of electrical currents flowing along the z-direction. This is readily accomplished by once again applying FDM to the Poisson equation and solving for the corresponding values of A_z as if they were voltage potentials. However, magnetic vector potential is more of a mathematical convenience than a useful physical quantity. The quantity we really desire to solve for is the magnetic field intensity $\mathbf{B}$. Applying the curl operation from Equation (59) in two dimensions therefore gives us

$$\mathbf{B}(\mathbf{r}) = \hat{\mathbf{x}} \frac{\partial A_z}{\partial y} - \hat{\mathbf{y}} \frac{\partial A_z}{\partial x} \ . \tag{69}$$

Note that this expression is analogous to the relation between voltage potential and electric field intensity as found in Equation (23). We may therefore define a similar grid stencil between A_z and $\mathbf{B}$ by using the convention shown in Figure 10.

References

[1] M. N. O. Sakidu, *Numerical Techniques in Electromagnetics*, 2nd ed. Boca Raton, Fl: CRC Press, 2001.

[2] P.-B. Zhou, *Numerical Analysis of Electromagnetic Fields.* Springer Verlag, 1993.

[3] W. H. Press, S. A. Teukolsky, W. T. Vetterling, and B. P. Flannery, *Numerical Recipes: The Art of Scientific Computing*, 3rd ed. Cambridge University Press, 2007.

[4] E. Haber, U. M. Ascher, D. A. Aruliah, and D. W. Oldenburg, "Fast simulation of 3D electromagnetic problems using potentials," *Journal of Computational Physics*, vol. 163, no. 1, pp. 150 – 171, 2000.